Colloids and Surfaces A: Physicochemical and Engineering Aspects 690 (2024) 133697

Contents lists available at ScienceDirect

Colloids and Surfaces A: Physicochemical and Engineering Aspects

journal homepage: www.elsevier.com/locate/colsurfa

Nanoparticle depressants in froth flotation – The effect of colloidal silica with different size and surface modifications on the selective separation of semi-soluble salt type minerals

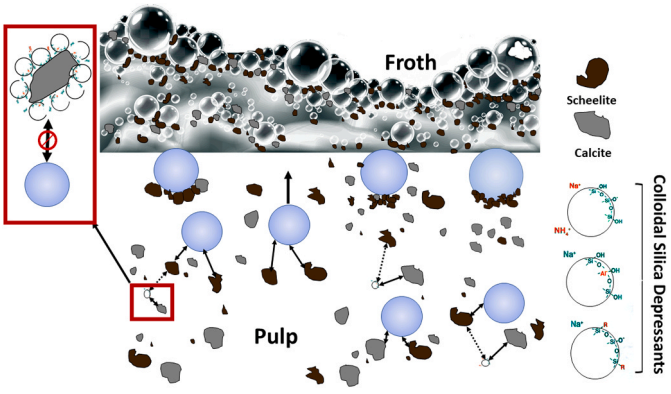
B. Ben Said [a,b,*], M. Rudolph [a], D. Ebert [a], D. Goldmann [b], L. Pereira [a]

[a] Helmholtz-Zentrum Dresden-Rossendorf, Helmholtz-Institute Freiberg for Resource Technology, Chemnitzer Straße. 40, Freiberg 09599, Germany
[b] Institute of Mineral and Waste Processing, Recycling and Circular Economy Systems, Walther-Nernst-Straße 9, Clausthal-Zellerfeld D-38678, Germany

HIGHLIGHTS

- Colloidal silica selectively inhibits the microflotation of calcite.
- Significant improvement in the scheelite-calcite selectivity in batch scale.
- The effect of colloidal silica is strongly dependent on its modification and size.
- Froth properties dependent on the colloidal silica type.
- The different effects are possibly due to the different aggregation mechanisms.

GRAPHICAL ABSTRACT



ARTICLE INFO

Keywords:
Scheelite
Calcite
Hornblende
Design of experiments
Surface charge
Hallimond tube
Batch flotation

ABSTRACT

Colloidal silica has been presented as a selective depressant in froth flotation separation of scheelite and calcite by our group in 2020. Here we analyze the effects of colloidal silica dosage, specific surface area (i.e. size), and modification with microflotation on pure scheelite, calcite, fluorite, and apatite minerals. In a reagents scale-up procedure batch flotation experiments were conducted on a low-grade scheelite ore using statistical experimental design methodology. Microflotation experiments showed colloidal silica selectively depressing calcite flotation with increasing intensity with reduced size of colloidal silica. The nanoparticulate depressant did not affect the recoveries of scheelite, apatite, and fluorite – typical ore minerals that occur associated with calcite. Batch flotation of a low-grade scheelite ore confirmed the observations made at the microscale: colloidal silica significantly improves the scheelite-calcite selectivity index. Here, we observe a series of relations between colloidal silica specific surface area and modification on different process indicators such as scheelite-calcite selectivity index, recoveries, and froth properties. These relations are assumed to be due to the different aggregation mechanisms of the colloidal silica dispersions. The aluminate-modified colloidal silica, which tends to form a coherent gel network in the presence of Ca^{2+}, shows the strongest effect on reducing calcite recovery

* Correspondence to: Department of Processing, Helmholtz-Institute Freiberg for Resource Technology, Helmholtz-Zentrum Dresden-Rossendorf, Chemnitzer Straße 40, Freiberg, Germany.
E-mail address: b.ben-said@hzdr.de (B. Ben Said).

https://doi.org/10.1016/j.colsurfa.2024.133697
Received 15 August 2023; Received in revised form 20 February 2024; Accepted 10 March 2024
Available online 13 March 2024
0927-7757/© 2024 The Authors. Published by Elsevier B.V. This is an open access article under the CC BY license (http://creativecommons.org/licenses/by/4.0/).

accompanied by a significant reduction in scheelite recovery compared to the non-functionalised and silane-modified colloidal silica.

1. Introduction

Froth flotation, a hetercoagulation separation process is considered the most widely used ore beneficiation process in mineral processing [1]. This process is based on the mineral surface specific ability of particles to adhere (i.e. attach and resistance to detachment) to gas bubbles. Flotation is generally described as a two-stage process in which valuable minerals are first introduced into the pulp zone, collected, and transferred to the froth zone together with entrained particles. Depressants are chemical reagents used to selectively inhibit the flotation of certain minerals or particles while allowing others to float. Depressants work by attaching to the surface of certain minerals and preventing them from interacting with the collector making them less likely to attach to air bubbles and float to the surface [1].Semi-soluble salt type minerals (SSSMs) are a group of minerals with similar surface properties [2]. These minerals often have Ca^{2+} cations at their surface, and their anions (CO_3^{2-}, F^-, WO_4^{2-}, and PO_4^{3-}) are close in size. These chemical properties translate into challenges for separating SSSMs from each other by means of froth flotation [2]. Resolving problems associated with the selectivity of SSSM flotation would directly translate into better raw materials efficiency.

To address this problem, various depressants were used such as sodium fluoride[3], phosphate[4], starch [4,5], tannins [4,5], and sodium silicate [4,6–10] for SSSM flotation. Recent studies aimed at checking the mechanisms and applicability of acidified sodium silicate as a calcite depressant [4,11–13]. Dong et al. [11] found that the chemisorption of acidified water on the calcite surface was greater than that of scheelite. Kupka et al.[14] showed that the effect of acidified water glass on calcite at microflotation scale depends on the acid used for its generation and the acidification degree. Besides, the authors found that its effect on scheelite-calcite selectivity in batch scale was lower than that of non-acidified water glass, in contrast to other studies [15,16], and indicated the main cause to be froth instability caused by acid addition.

Recently, our group introduced the approach to directly applying colloidal silica (CS) as a potential depressant in the flotation of scheelite [10]. This short communication presented preliminary findings which had been limited to the microflotation experiments with pure scheelite and calcite and only a few batch flotation tests with unsystematic variations of colloidal silica properties.

Colloidal silica formulations have a wide range of applications due to their unique properties [17,18]. The stability of colloidal silica is critical for controlling particle dispersion and preventing agglomeration. It can be stabilized by ionic charge or adsorption of molecules or polymers [17]. Some examples of functional groups or coatings that can be used to stabilize colloidal silica are aluminate and silane. When colloidal silica is modified with aluminate, the surface acquires a constant negative charge that is less pH dependent at a higher absolute compared to unmodified silica [17–19]. The pH value also influences the stability of colloidal silica, as it affects the surface charge and electrostatic interactions [17]. Aggregation can occur in the form of gelation, coagulation, or flocculation and is influenced by pH, particle size, concentration, temperature, and dissolved ionic species [17].

This study covers a more thorough investigation of the application of colloidal silica as a calcite depressant in SSSM flotation. The effects of pH and colloidal silica dosage, modification, and specific surface area (SSA) on the flotation of scheelite, fluorite, apatite, and calcite are investigated in micro scale. Besides, the flotation of a low-grade scheelite ore is investigated in batch flotation scale using a statistical design of experiments (DoE) approach [20], in which the effect of collector dosage, pH, and colloidal silica dosage, specific surface area, and modification are investigated. The goals of this investigation are two-fold: identify the significance of the different process parameters on grades, recoveries, selectivity indices, and froth properties; construct hypotheses for the mechanisms controlling the flotation of SSSM after the addition of colloidal silica, which can later be evaluated with fundamental investigations.

Table 1
Summary of colloidal silica suspensions and their specifications. *calculated from the specific surface area **investigated only in microflotation.

Specific surface area ($\frac{m^2}{g}$)	Modification (-)	Particle size* (nm)	Acronym
250	None	9	N_250
500	None	4.5	N_500
750	None	3.2	N_750**
220	Silane	10	S_220
500	Silane	4.5	S_500
250	Aluminate	9	Al_250
500	Aluminate	4.5	Al_500
1100	Aluminate	2	Al_1100

2. Material and methods

2.1. Reagents

The collector used was sodium oleate $C_{18}H_{33}NaO_2$ (NaOl) from Carl Roth with a purity of 90%. pH modifiers are hydrochloric (HCl) acid and sodium hydroxide (NaOH) from Carl Roth GmbH, and frother is 4-methyl-2-pentanol (MIBC) supplied by Alfa Aesar. Eight types of Levasil® Colloidal Silica (CS) provided by Nouryon were tested as calcite depressants, differing in modification and specific surface area, as summarized in Table 1.

2.2. Design of experiments

Statistical Design of Experiments (DoE) [21] is a systematic approach to understanding the relationships between input factors (independent variables) and response variables (dependent variables) using the smallest possible number of experiments. A full factorial experimental design is used for the experimental design of batch and microflotation. Significant factors and their interactions are identified. The effect E of a process parameter is defined as the difference between the mean value of the target variable with level (+) and the mean value of the target variable with level (-) divided by two. The interaction is calculated similarly.

2.3. Micro floatation experiments

2.3.1. Pure minerals

Pure minerals of scheelite, calcite, apatite, and fluorite were used in microflotation. To obtain a similar range of settling velocities, the minerals were ground and dry sieved to a specific target size fraction, as a function of their densities. The settling velocities were calculated following Stoke's law for the middle size of the fraction. X-ray powder diffraction (XRD) analyses were performed on a PANalytical Empyrean diffractometer with Co radiation at a voltage of 35 kV and a current of 35 mA. According to the results of the XRD analysis (Table 2), all minerals are highly pure.

2.3.2. Experimental procedure

One gram of each mineral was added to 160 ml of KCl and the mixture was stirred at 400 rpm in a beaker with a magnetic bar. The pH

Table 2
Minerals used in microflotation, settling velocities calculated following Stoke's law for the middle size of the fraction.

Mineral	Source	Impurity	Purity (%)	Size fraction (μm)	Density ($\frac{g}{cm^3}$)	Settling velocity ($\frac{m}{s}$)
Scheelite	Mittersill Austria	Mica	98.2	32–63	6.12	$6.23 * 10^{-6}$
Calcite	Brilon Sauerland Germany	Quartz	99.6	63–100	2.71	$6.18 * 10^{-6}$
Apatite	Minas Gerais Brasil	Quartz	99.0	63–80	3.18	$6.07 * 10^{-6}$
Fluorite	China	Quartz	99.5	63–80	3.18	$6.07 * 10^{-6}$

Table 3
Investigated parameters and parameter levels of microflotation tests (2^2 full factorial design).

Parameter	Unit	Factor level	
		minimum	maximum
pH	-	8	10
Collector dosage	mol/L	10^{-3}	
Depressant dosage	mg/L	0	100

of the slurry was adjusted with 1 M HCl or NaOH feedstock solutions, with two minutes of conditioning time. Following pH stabilization, depressant and collector conditioning were performed in sequence, each done for three minutes at 400 rpm. Next, the suspension was transferred to the Hallimond tube and stirred for 2 minutes at 800 rpm. Microflotation lasted two minutes at an airflow rate of 20 cm^3/min. The collected concentrates and tailings were filtered and dried overnight at 50–60 °C.

Two experimental stages were conducted. In the first stage, the target lay in identifying the depressing effect of colloidal silica on all minerals, microflotation tests of scheelite, calcite, apatite and fluorite were carried out at pH 8 and 10^{-3} mol/l sodium oleate concentration, with colloidal silica dosages varying from 0 mg/l to 200 mg/l. In the second stage, the target was investigating in depth the influence of colloidal silica as a calcite depressant, tests were carried out with a full factorial design of experiments approach. Process parameters were pH and colloidal silica dosage, modification, and specific surface area. Table 3 shows the experimental design applied for each of the colloidal silica suspensions (c.f. Table 1). In both experimental batches, three repetitions were performed for each test.

2.4. Batch flotation experiments

2.4.1. Ore and overall flotation procedure

The low-grade scheelite ore investigated comes from an active mine exploiting a stratabound deposit and contains 0.5% (w/w) scheelite and 1.1% (w/w) calcite. The main gangue minerals are hornblende, plagioclase, and quartz, which together account for 77.5% (w/w) of the ore, as illustrated in Fig. 1. Ore samples were collected in the processing plant directly after the final milling stage, being its particle size distribution suitable for flotation ($d_{80,3}$ = 150 μm). Aliquots of 500 g were split using Retsch PT100 to be used as feed for each test. Before each flotation test, the ore was added to 300 ml of water and ground in a laboratory scale rod mill for 3 minutes at 96 rpm to reactivate particle surfaces. Froth flotation tests were performed in a Magotteaux® bottom-driven flotation cell at 33% pulp density, 450 rpm impeller speed, and 5 l/min air flow rate. The conditioning scheme is illustrated in Fig. 2.

Three concentrates were collected within [0; 60] s, [60; 180] s, and [180; 420] s time intervals. The froth was scraped in 5 s intervals. The filtered flotation products were dried overnight at 50 °C to 60 °C in a

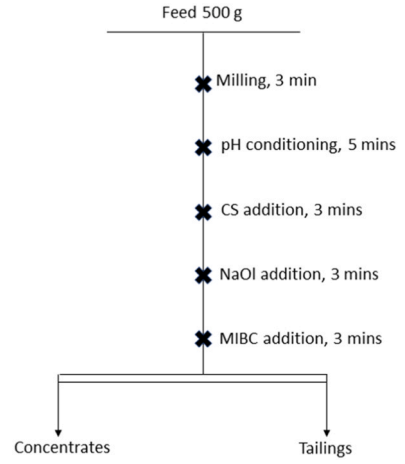


Fig. 2. Flotation flow chart of low grade scheelite ore.

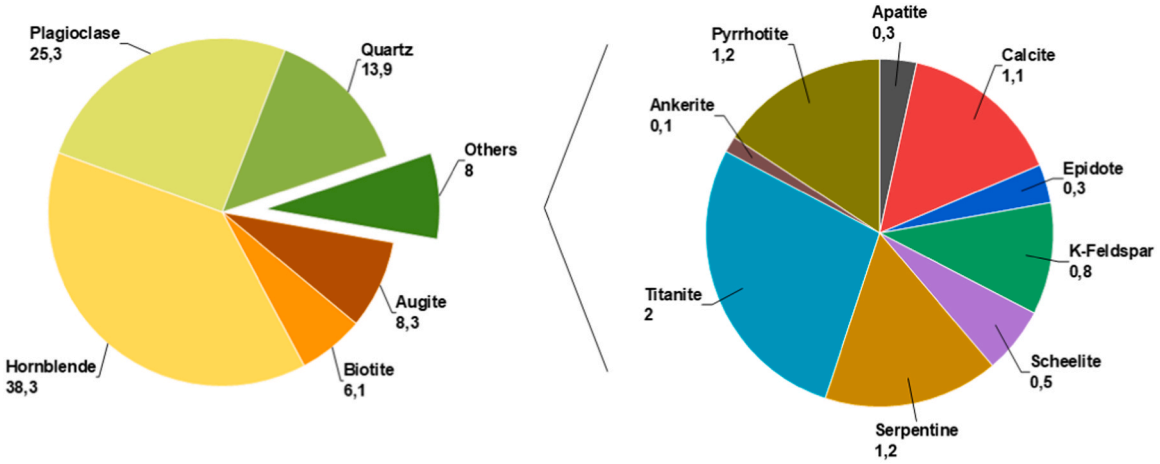


Fig. 1. Mineralogical composition of the ore in % (w/w) obtained by X-ray diffraction (XRD) and mineral liberation analyser (MLA).

Table 4
Levels of variables investigated for the blank tests (2^2 full factorial design).

Parameter	Unit	Factor level	
		minimum	Maximum
pH	-	8	10
Collector dosage	g/t	100	400

Table 5
Levels of variables investigated for the tests with colloidal silica (2^3 full factorial design). These process conditions were applied separately to each of the colloidal silica modifications (c.f. Table 1).

Parameter	Unit	Factor level	
		minimum	Maximum
pH	-	8	10
Collector dosage	g/t	100	400
Depressant dosage	g/t	50	550

Table 6
Investigated variables and their levels in the 2 full factorial design. This experimental design is a combination of results from the second experimental batch (c.f. Table 5).

Parameter	Unit	Factor level	
		minimum	Maximum
pH	-	8	10
Collector dosage	g/t	100	400
CS dosage	g/t	50	550
CS specific surface area	m^2/g	250	500
CS modification (silane or aluminate)	-	no	Yes

drying oven, and mass recoveries were calculated based on dry weights. All samples were split and then analyzed with a Bruker S1 TITAN 800 portable XRF (pXRF). Some samples were analyzed with XRD and the mineral liberation analyzer (MLA) [22] so that pXRF results could be converted into mineralogical compositions based on an element-to-mineral-conversion methodology, which is described in Appendix I.

2.4.2. Experimental conditions

Experiments were conducted using a full factorial design of experiments approach [21]. Two experimental stages were conducted. In the first stage (Table 4), which can be considered as the blank test for reference, pH, and sodium oleate dosage were the variables. In the second stage (Table 5), which was performed for each colloidal silica suspension and was aimed at investigating the effect of colloidal silica dosage, pH, sodium oleate dosage, and colloidal silica dosage were the process parameters. The experimental design illustrated in Table 6 is a combination of results from the second experimental batch so that the effect of colloidal silica specific surface area and modification are highlighted. Here pH, sodium oleate dosage, and colloidal silica dosage, modification, and specific surface area were variable.

The results were analyzed using an in-house developed shiny R platform that allows, among other things, to design and evaluate an experimental plan, computing the main and interaction effects of the process parameters as well as their statistical significance. This platform is open-access and can be accessed in [23].

2.4.3. Froth investigation

During all batch flotation experiments, a froth image was taken every second at the side of the flotation cell, as displayed in Fig. 3. Bubbles were identified in these pictures using the *SimpleBlobDetector* function of openCV in python [24] and their size and position were used for the statistical evaluation of froth properties using R [25].

2.5. Zeta potential measurements

Zeta potentials of colloidal silica suspensions were determined from electroacoustic and ultrasonic attenuation measurements using the Colloidal Dynamics AcoustoSizer II for dilute particle suspensions. Dilute colloidal silica suspensions were prepared at 0.5% (w/w) solids, in 10^{-2} M KCl and dispersed with a magnetic stirrer for 10 min. The suspension pH was altered to a desired value with HCl and NaOH solutions and left to equilibrate for 10 min before the samples were directly injected into the mixer for zeta potential measurements. The measurements were performed over the pH range [2; 11].

3. Results

3.1. Micro flotation and link to surface charge

The effect of colloidal silica dosage on the microflotation recoveries of calcite, scheelite, fluorite, and apatite at a sodium oleate concentration of 10^{-3} mol/l, pH 8, and a specific surface area of colloidal silica of 500 m^2/g are shown in Fig. 4. It can be seen that colloidal silica depress calcite. In contrast, the recoveries of scheelite, fluorite, and apatite are not affected by the reagent, irrespective of its modification. Moreover, at a specific surface area of 500 m^2/g, silane-modified colloidal silica shows the strongest depressive effect on calcite, followed by unmodified

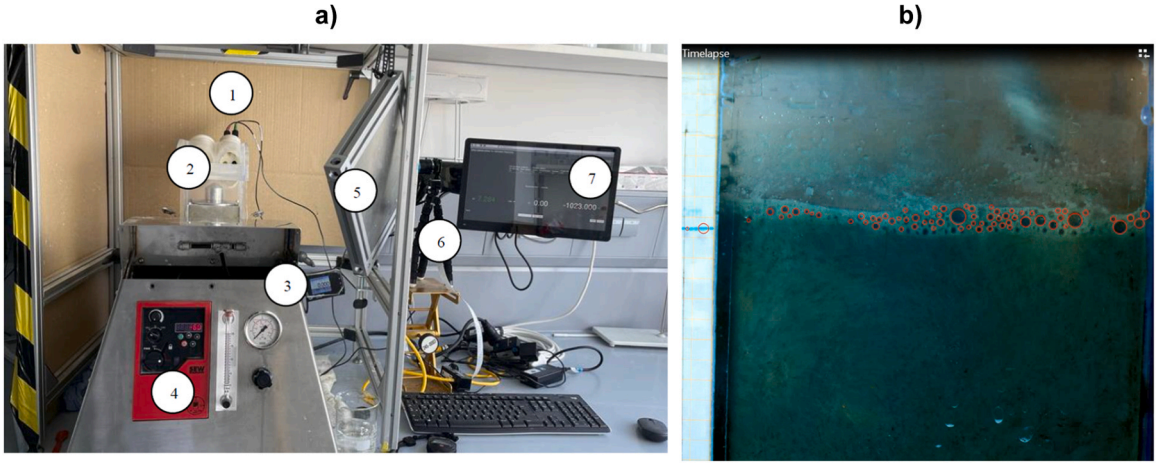


Fig. 3. (a) Batch flotation system with 1) pH and conductivity probes, 2) flotation cell, 3) airflow controller, 4) speed controller, 5) lighting, 6) froth camera, 7) Raspberry system and (b) recorded froth picture with bubbles detection.

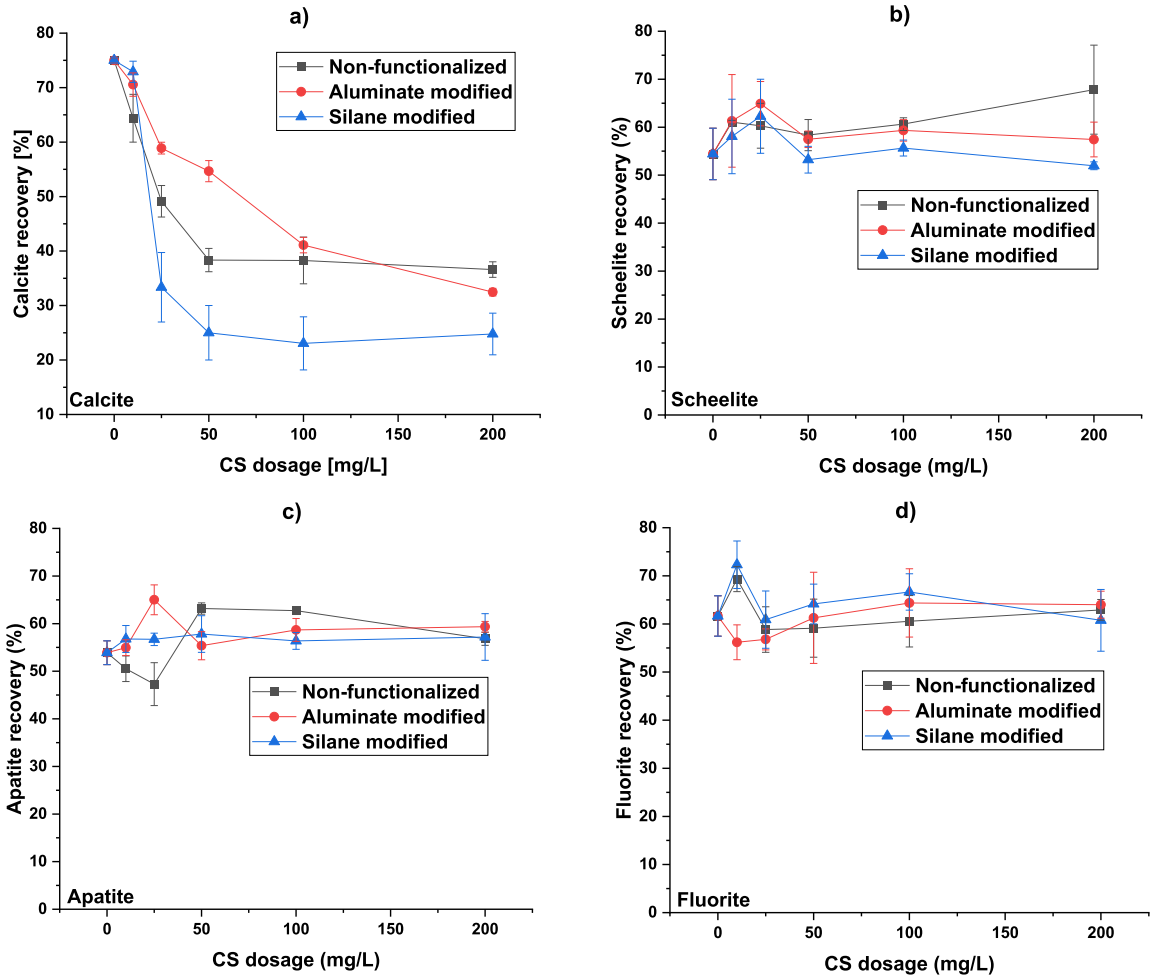


Fig. 4. Single-mineral flotation recoveries of calcite, scheelite, apatite, and fluorite depending on colloidal silica dosage (at pH = 8, collector = $1 * 10^{-3}$ M sodium oleate, specific surface area 500 m^2/g).

and aluminate-modified colloidal silica. Besides, Fig. 5 shows the direct relation between CS specific surface area and the depression of calcite, again irrespective of the colloidal silica modification. Increasing the specific surface area leads to a decrease in calcite recovery for the three colloidal silica types.

Fig. 6 shows the effects of pH and its interactions with the dosage and the specific surface area of colloidal silica on calcite recovery. The dependence of the pH effect on the dosage and specific surface area of the colloidal silica is more pronounced for the silane-modified colloidal silica. Fig. 7 shows the interaction diagrams of the pH with the dosage and the specific surface area of colloidal silica. For both modifications, the effect of pH depends on the dosage of colloidal silica: If no colloidal silica is used, the pH does not affect calcite recovery. With a dosage of 100 mg/l colloidal silica, the calcite recovery increases when the pH is raised from 8 to 10 (Fig. 7a and b). The interaction of pH with the specific surface area is less pronounced (Fig. 7c and d), with a stronger correlation for both modifications at pH 8 and a specific surface area of 500 m^2/g.

Zeta potential results based on the electroacoustic measurements are shown in Fig. 8. For the non-functionalized and the silane-modified colloidal silica, the isoelectric point is around pH 2–4. The surface charge of the aluminate-modified colloidal silica is negative throughout the observed pH range. These findings are consistent with previous work [18,26]. From the graph, it can be seen that the zeta potentials of the colloidal silica suspensions with a specific surface area of 220 m^2/g to 250 m^2/g in the pH range of 8–10 are close and vary between −25 mV and −12 mV. This variation is more pronounced and pH-dependent at a specific surface area of the colloidal silicas of 500 m^2/g. At pH 8, the absolute deviation of the zeta potentials of the two functionalized colloidal silicas is 33 mV. At pH 10, this absolute deviation decreases to 11 mV. This might relate to the joint influence of specific surface area and pH on calcite recovery.

3.2. Batch flotation

3.2.1. Effect on calcite and scheelite recovery

The effect of colloidal silica dosage for the different CS dispersions in comparison to the blank tests on calcite recovery is shown in Fig. 9a, where an increase in the dosage of colloidal silica leads to a decrease in calcite recovery. These results agree with observations made for microflotation experiments. The effect of colloidal silica dosage, which can be seen in Fig. 9b, is almost the same in the case of the non-functionalized and silane-modified colloidal silica. In the case of the aluminate-modified colloidal silica, this effect is more pronounced. As for the effects of NaOl dosage and pH, it is clear that they are more pronounced in the silane-modified colloidal silica. An increase in specific surface area leads to a decrease in calcite recovery for all three colloidal silica types, but this effect is more pronounced for the functionalized colloidal silicas.

The effects of colloidal silica dosage for the different suspensions on scheelite recovery are shown in Fig. 10a. It can be seen that varying colloidal silica dosage from 50 g/t to 550 g/t negatively affects scheelite recovery for all CS dispersions used but the aluminate-modified CS with of 1100 m^2/g SSA, for which the impact in scheelite recovery is very

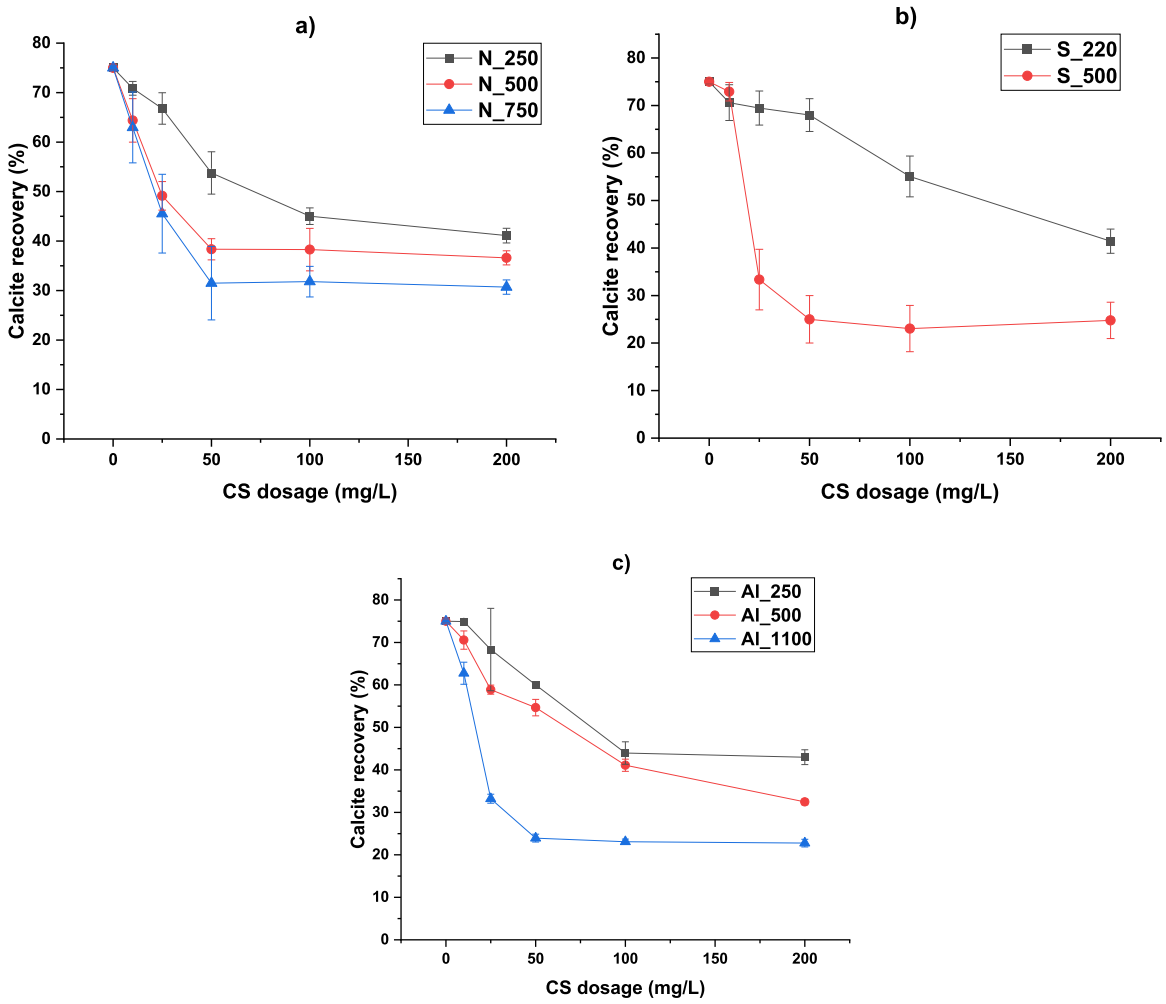


Fig. 5. Single-mineral flotation recoveries of calcite depending on colloidal silica dosage.

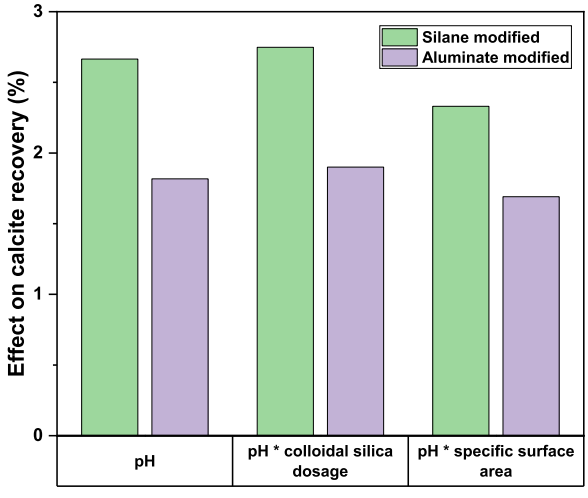


Fig. 6. Effects of process parameter pH and its interactions with the dosage of colloidal silica and the specific surface area on calcite recovery in microflotation.

similar at low and high CS dosages. Moreover, increasing SSA hinders scheelite recovery, especially at higher colloidal silica dosage.

NaOl dosage and pH have a positive effect on scheelite recovery for all colloidal silica types (Fig. 10b). Compared to the non-functionalized colloidal silica, the silane modification has a more pronounced negative effect on scheelite recovery and seems to be less affected by the increase in specific surface area. The aluminate modification, on the other hand, hinders scheelite recovery significantly, especially with an increase in specific surface area.

These observations are in contrast to the microflotation experiments, where no significant difference was found between the effects of functionalization of the three colloidal silica suspensions on scheelite recovery. This contrast points out the effects of colloidal silica in different flotation sub-processes.

While microflotation observations have shown that silane-modified colloidal silica has a strong depressing effect on calcite at a specific surface area of 500 m^2/g (c.f. Fig. 4a), the experiments in batch flotation show aluminate modification having the strongest effect on calcite recovery reduction.

This suggests that the colloidal silica depressants also have a strong (modification, pH and colloidal size dependent) effect on the recovery-relevant micro-processes, which are not present in microflotation and which can be found in:

(i) the froth phase, e.g. drainage behavior, bubble coarsening, and bubble loading as well as,
(ii) in the pulp zone, e.g. turbulent bubble formation and stabilization, complex dissolution/precipitation dynamic non-equilibria between the different phases composing the particles, frother interactions, and pulp rheological effects.

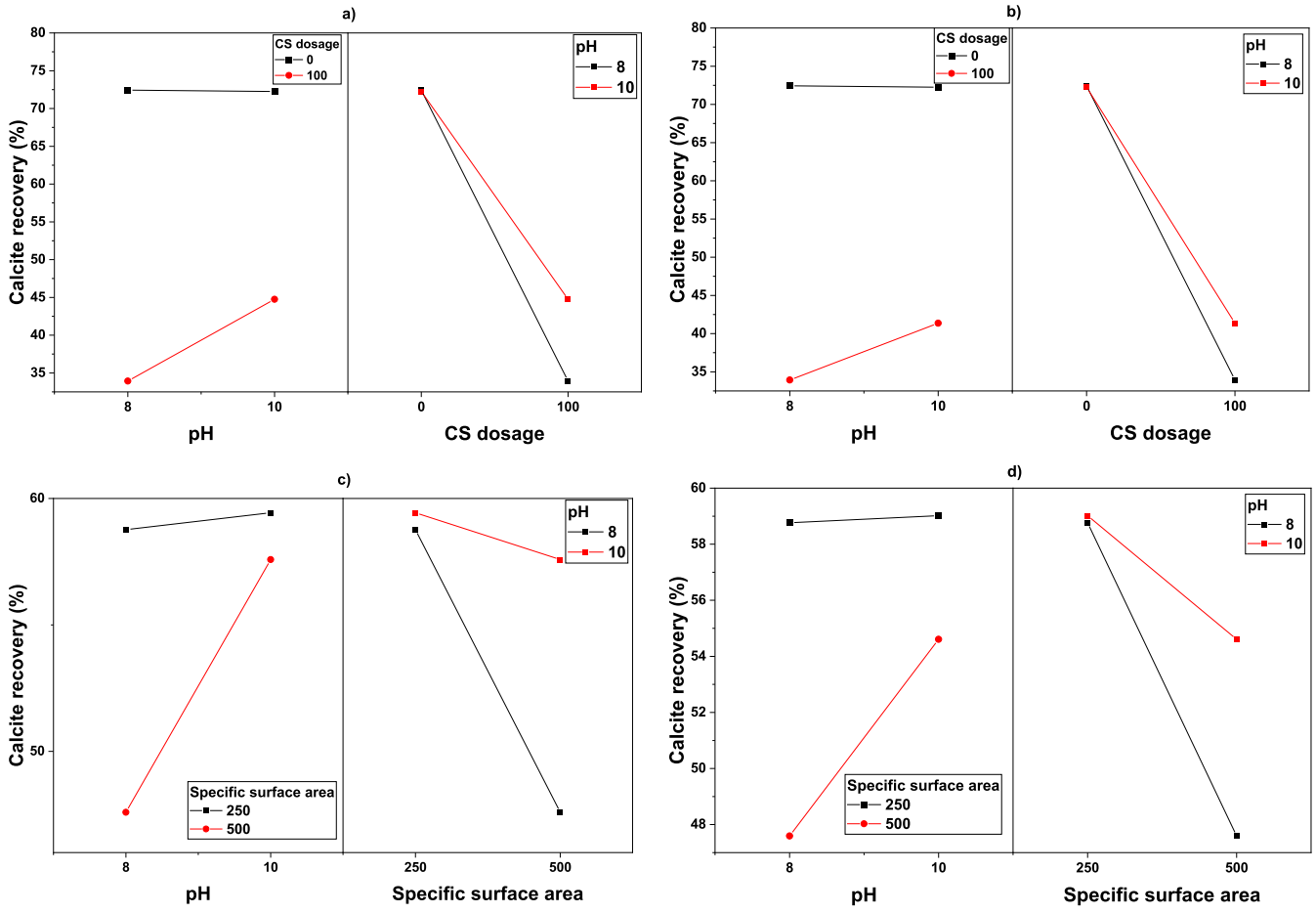


Fig. 7. Interaction plots of pH and CS dosage for the silane (a) and aluminate (b) modified colloidal silica and of pH and SSA for the silane (c) and aluminate (d) modified colloidal silica.

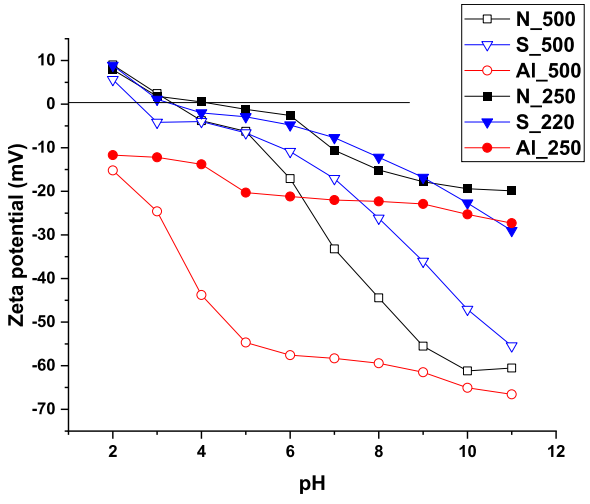


Fig. 8. Zeta potential for the different types of colloidal silica (cf. Table 1) at different pH, obtained by measuring the dynamic electrophoretic mobility in an electroacoustic analysis.

3.2.2. *Selectivity index*

The effect of colloidal silica dosage for the different colloidal silica dispersions on the scheelite-calcite selectivity index is shown in Fig. 11. It is obvious that all colloidal silica dispersions positively affect the selectivity of scheelite against calcite in this case study, with the highest selectivity obtained with a high dosage of the smallest aluminate functionalized nanoparticles (Al_1100).

Although the aluminate-modified colloidal silica showed the strongest depressing effect on calcite (highest selectivity against calcite), the fact that this effect reached a significant decrease in the scheelite recovery makes the difference in the effects on the selectivity index compared to the non-functionalized and the silane-modified colloidal silica is not significant.

3.2.3. *Effect on calcite and scheelite grade*

Fig. 12a shows that all colloidal silica dispersions show a negative effect on calcite grade in the concentrate as compared to the blank tests. Increasing the colloidal silica dosage from 50 g/t to 550 g/t leads to a further decrease in calcite grade. The aluminate modification shows the strongest effect on calcite grade reduction than that of the non-modified colloidal silica, while the opposite is observed for the silane modification (Fig. 12b).

Scheelite grade is also negatively impacted by the use of colloidal silica (Fig. 12c). Hence, considering the effects of CS on gangue minerals other than calcite is required for understanding these results.

From the plot of the effects on hornblende recovery (an abundant mineral in the tested ore) (Fig. 12e) it is evident that the aluminate modification impairs hornblende flotation the most. This helps explain why, even though the aluminate modification highly hinders scheelite recovery (Fig. 10b), a grade similar to the non-functionalized and silane-modified colloidal silica is still achieved. Furthermore, the pronounced effect of the aluminate modification and its SSA on the recovery of this hydrophobic mineral is observed, which points out the need to

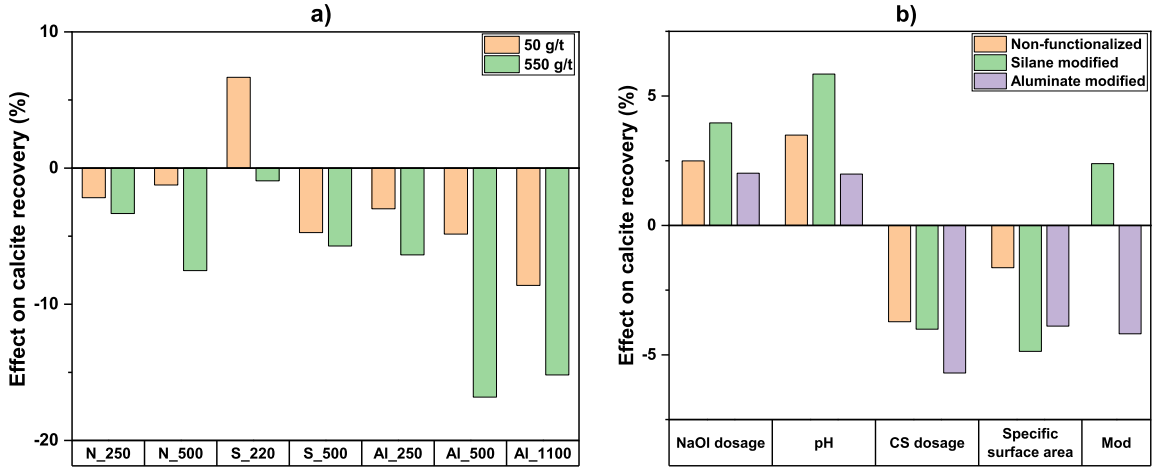


Fig. 9. Effects on calcite recovery of colloidal silica dosage in comparison to blank tests for seven types of colloidal silica suspensions according to the experimental design in the second (a) and third (b) experimental batches (c.f., Table 5 and Table 6, respectively).

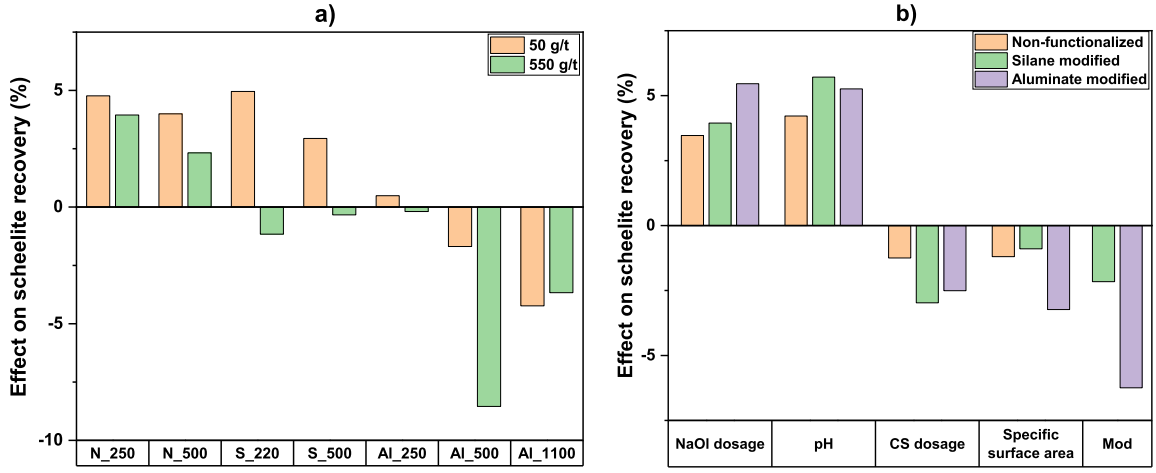


Fig. 10. Effects on scheelite recovery of colloidal silica dosage in comparison to blank tests for seven types of colloidal silica suspensions according to the experimental design in the second (a) and third (b) experimental batches (c.f., Table 5 and Table 6, respectively).

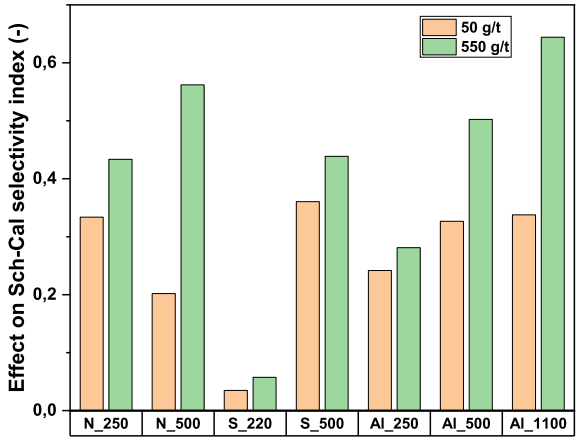


Fig. 11. Effects on scheelite-calcite selectivity index of colloidal silica dosage in comparison to blank tests for seven types of colloidal silica suspensions according to the experimental design in Table 3.

understand the role of colloidal silica on froth properties.

3.3. Froth properties

3.3.1. Froth loading

The mass pull versus water pull diagrams of batch flotation tests at different parameter settings (c.f. Table 5) in Fig. 13 show that the froth is least loaded with the aluminate-modified colloidal silica. Moreover, in contrast to the aluminate-modified colloidal silica, both the non-functionalized and the silane-modified colloidal silica show a strong linear relationship between water pull and mass pull at a specific surface area of 220–250 m^2/g. However, at a specific surface area of 500 m2/g, for both the non-functionalized and the aluminum-modified colloidal silica, a linear relationship between water pull and mass pull is observed.

This change in the relationship between mass and water pull for the three colloidal silica types supports the fact that the colloidal silica depressants also have a strong modification and specific surface area dependent effect on the micro-processes relevant to mass and water pull. Fig. 14 further clarifies this aspect. When compared to the non-modified CS, the aluminate-modified CS leads to higher water pull and smaller mass pull which means a wetter Froth. On the other hand, the silane modification reduces both mass and water pull in comparison to the

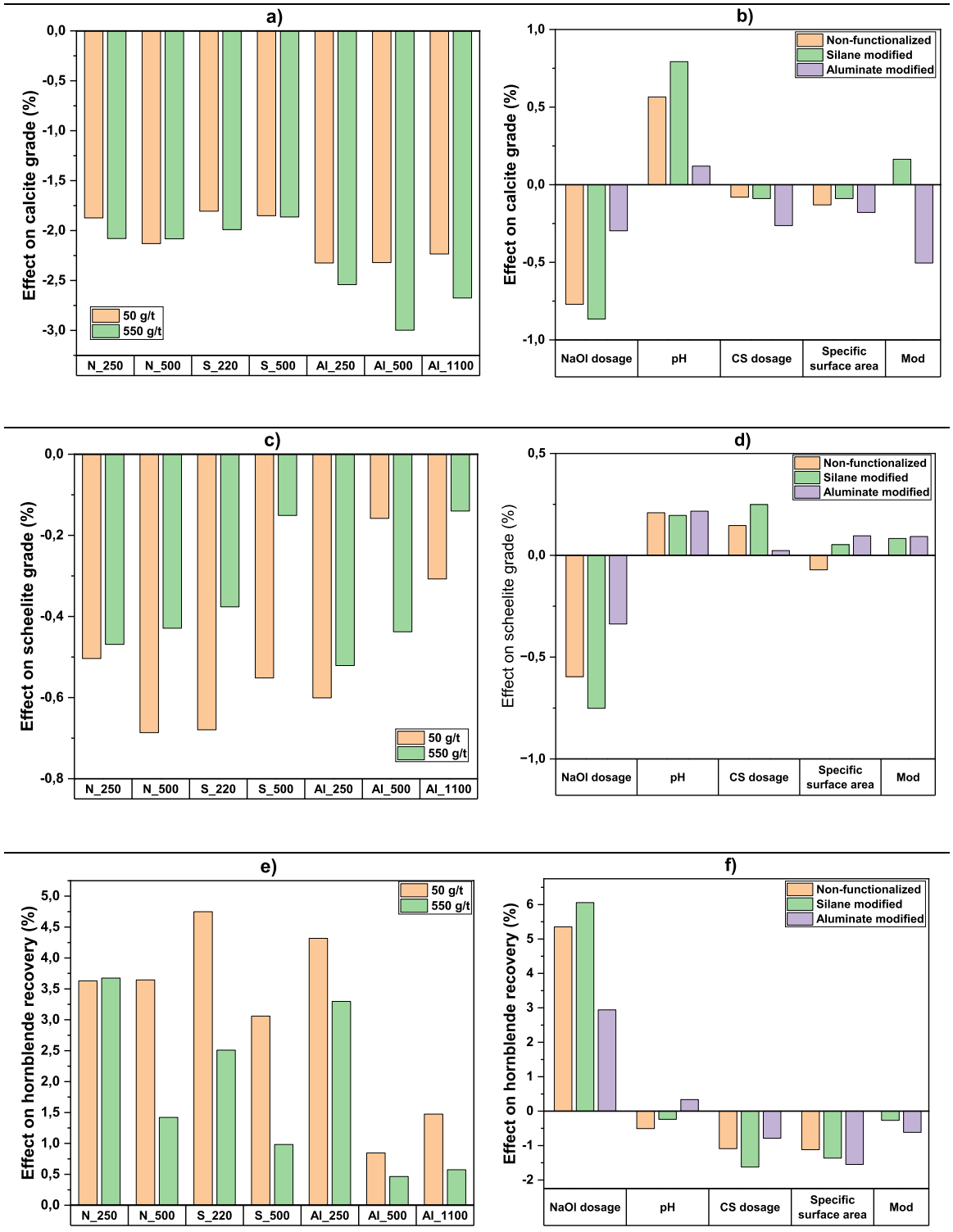


Fig. 12. Effects of colloidal silica dosage in comparison to blank tests for seven types of colloidal silica suspensions according to the experimental design in Table 3 (left) and of the process parameters according to the experimental design in Table 4 (right) on calcite grade (a and b), scheelite grade (c and d) and hornblende recovery (e and f).

non-modified CS, thus not significantly changing froth characteristics.

In the case of the functionalized colloidal silicas, their SSA negatively affect both mass and water pull, with the effect being more pronounced for the aluminate-modified CS. In contrast, the role of SSA is different for the non-functionalized colloidal silica, with almost no effect on water pull and a negative effect on mass pull. As a result, the specific surface area of functionalized and non-functionalized colloidal silica should affect froth loading and, consequently, froth characteristics in opposite ways. Such differences may be due to two causes, which may occur singly or both simultaneously: On one side the modification type impacts froth stability via different phenomena occurring in the froth zone (e.g., water drainage and particle drop back), In the other hand, it is a result of sub-processes that take place in the pulp zone, which lead to different attachment rates/bubble loading and consequently changes

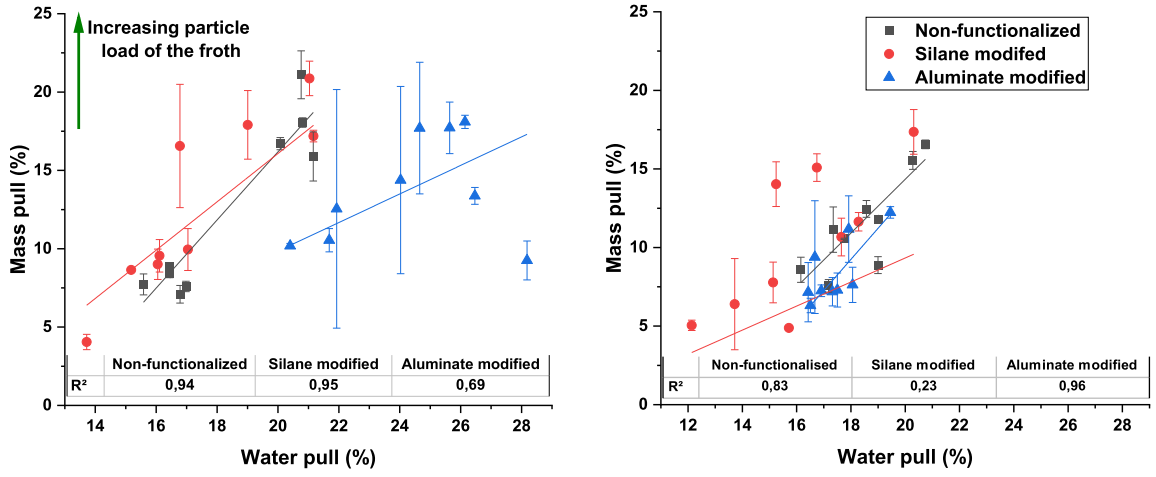


Fig. 13. Mass pull against water pull for the three types of colloidal silica at a specific surface area of 220–250 $\frac{m^2}{g}$ (left) and 500 $\frac{m^2}{g}$ (right).

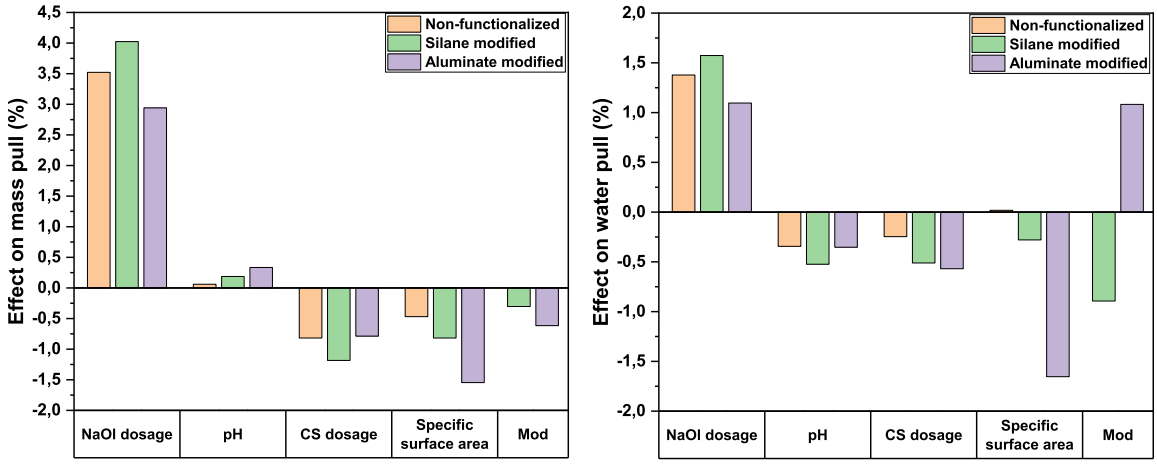


Fig. 14. Effects of the process parameters according to the experimental design in Table 4 on mass pull (left) and water pull (right).

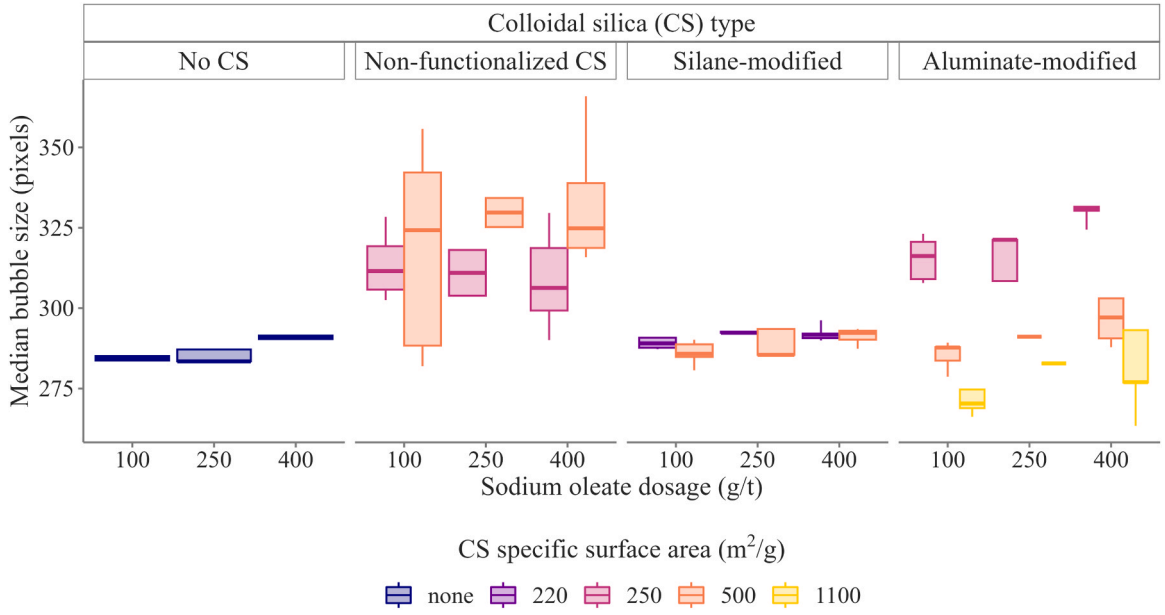


Fig. 15. Boxplots of median froth bubble size for blank tests and tests with the different colloidal silica suspensions at different colloidal silica dosages.

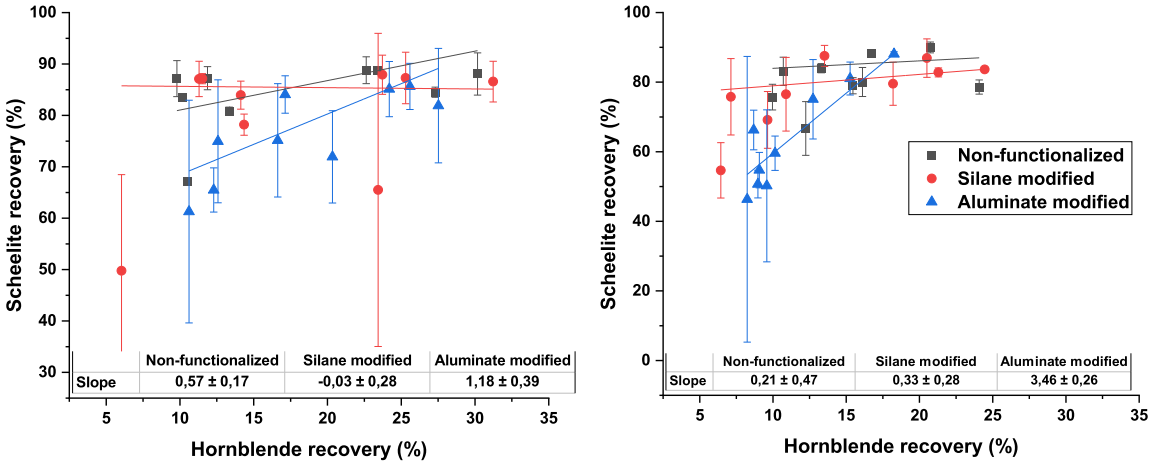


Fig. 16. Scheelite against hornblende recovery for the three types of colloidal silica at a specific surface area of 250 $\frac{m^2}{g}$ (left) and 500 $\frac{m^2}{g}$ (right).

Table 7
List of minerals.

Minerals	Contained elements	Subgroup name
Calcite	Ca	Calcite
Scheelite	Ca, W	Scheelite
Apatite	Ca, P	Apatite
Ankerite	Ca, Fe, Mg, Mg, Mn	Ankerite
Biotite, Muscovite, K-Feldspar	K, Mg, Fe, Al, Si	Biotite
Actinolite, Adanagaite, Zoisite/ Pumpellyite	Ca, Fe, Mg, Al, Si	Hornblende
Chamosite, Clinochlore	Fe, Mg, Al, Si	Chlorite
Albite, Plagioclase, Augite, Serpentine, Epidote	Ca, Al, Si	Albite
Talc	Mg, Si	Talc
Quartz	Si	Quartz
Titanite	Ca, Si. Ti	Titanite

Table 8
Ratio between minerals in each subgroup.

	Adanagaite/Zoisite	Actinolite/Zoisite	Biotite/Muscovite
Concentrate 1	3.77	0.48	16.35
Concentrate 2	3.77	0.44	21.17
Concentrate 3	4.05	0.45	22.74
Tailings	4.93	2.15	9.33

both mass and water recovery.

3.3.2. *Bubble size distributions in the froth zone*

Fig. 15 illustrates with boxplots the role of colloidal silica type and SSA on froth median bubble size. As can be observed, the froth bubble size is smaller with the silane-modified than with the unfunctionalized CS. Besides, SSA does not affect froth bubble size in the case of the silane modification. While bubble size decreases with an increase of SSA for the aluminate modification, the opposite is observed for the non-functionalized CS. There is a clear correlation here between the mass/water pull ratio and the median bubble size for each colloidal silica suspension, with the median bubble size being smaller for aluminate-modified colloidal silica which provides the less loaded froth in comparison to the non-functionalized and silane-modified colloidal silica. Morar et al. [27] show how particle loading affects froth bubble size. Smaller bubbles indicate smaller particle loading. This, however, is unable alone to explain the effect of CS modification and SSA on froth bubble size. The chemical properties of each colloidal silica type are likely to also play a significant role.

3.4. *Pulp zone vs. froth zone effects*

The depressing effect of colloidal silica on calcite by true flotation is supported by the results of microflotation experiments, where this effect became stronger with increasing specific surface area, and smaller size of the colloidal silica depressants. Since no firm conclusions can be drawn, further research is required to understand the mechanism of colloidal silica selectively adsorbing on the surface of calcite. This effect could be evaluated by the topography of the calcite's surface or by the interaction between the chemical specifications of each modification and the other reagent system parameters. Nevertheless, the large differences in the roughness of the calcite surface compared to other minerals do not preclude the roughness from playing an important role in the overall mechanism. Other differences, such as in lattice parameters or solubility, which would affect pulp chemistry, could also be responsible for this effect.

When comparing the behavior of the three types of colloidal silica at batch scale, it is noticeable that non-functionalized colloidal silica and silane show similar behavior concerning the target variables mass pull, water pull, scheelite recovery, calcite recovery, and hornblende recovery. However, in terms of froth properties, silane-modified colloidal silica differs from non-functionalized and aluminate-modified colloidal silica. This difference is key for developing a hypothesis about the microprocesses governing the impact of each colloidal silica modification. In the area of colloidal silica chemistry and its applications, the processes of silica nanoparticle aggregation and stability are of utmost significance. It is hypothesized that this process helps explain observations made in batch flotation.

There is a notable difference between the non-functionalized and silane-modified colloidal silica on the one hand and the aluminate-modified colloidal silica on the other when comparing the curves of the scheelite recovery against the Hornblende recovery in Fig. 16. At a specific surface area of 500 m^2/g and in the case of aluminate-modified colloidal silica, the recoveries of the two minerals are linearly related while on the other hand, the lines were almost horizontal for the colloidal silica that had not been functionalized or silane-modified. Decreasing the specific surface area to 250 m^2/g decreased the slope for the aluminate-modified colloidal silica while the slope of the non-functionalized colloidal silica increased slightly.

Given the instability of the two dispersions at high pH, which may be caused or at least enhanced by the presence of multivalent cationic species in the slurry, we propose that the aluminum-modified and the non-functionalized colloidal silica underwent aggregation in different ways. We hypothesize that the aluminate-modified colloidal silica

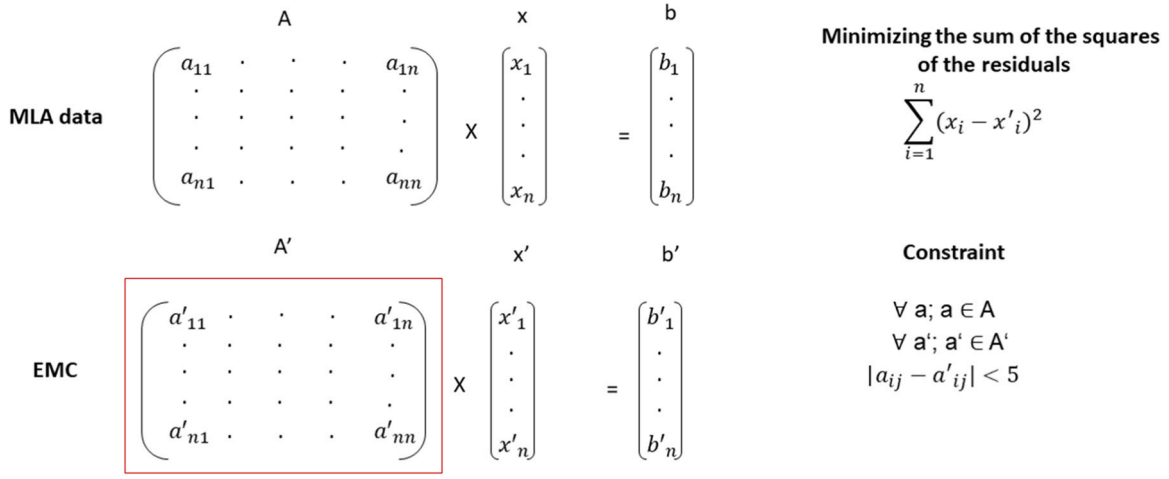


Fig. 17. Solver used for calculation of the conversion matrix.

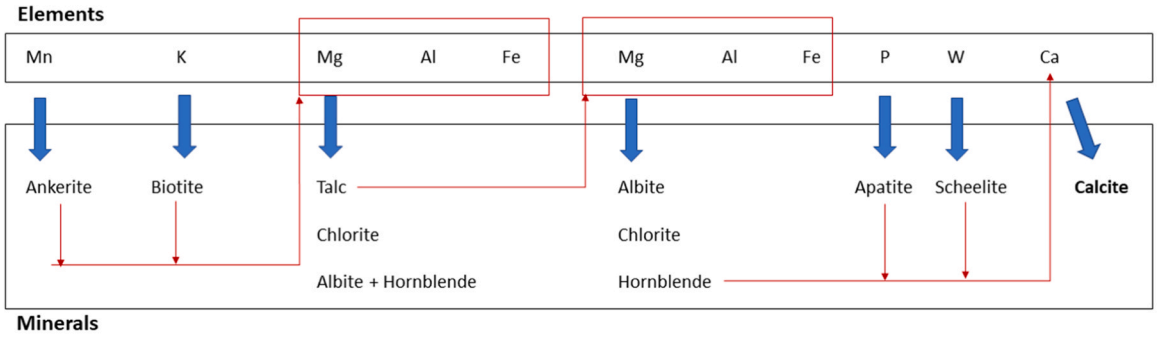


Fig. 18. Developed conversion scheme.

Table 9
Steps for the element to mineral conversion.

Step	Mineral computed	Elements used	Impacted elements
1	Ankerite	Mn	Ca, Fe, Mg, Mg
2	Biotite	K	Mg, Fe, Al, Si
3	Talc, Chlorite, (Hornblende and Albite)	Mg, Al, Fe	Si
4	Chlorite, Albite, Hornblende	Mg, Al, Fe	Ca, Si
5	Apatite	P	Ca
6	Scheelite	W	Ca
7	Calcite	Ca	

aggregate in gel form with a higher specific surface area leads to an increase in local pulp viscosity, reducing the bubble-particle collision efficiency for scheelite particles as the particles have lower mobility. This could affect their ability to move and redistribute within the tank and affect the concentration profile of the slurry so that the bottom regions of the cell have higher solids concentrations, reducing the number of hornblende particles that can be transported to and through the pulp-froth interface. It is known that the pulp-froth interface is crucial for the flotation process, as considerable amounts of the particles detach from the bubbles in this area. Kirjavainen showed a strong dependence of the entrainment of hydrophilic quartz and phlogopite on the viscosity of the suspension [28]. Amorphous silica was shown to have a greater effect on slurry viscosity in copper flotation than quartz, especially at high solids concentrations. This is because hydrogen bonds between silanol groups on adjacent silica units cause the formation of networks of amorphous silica particles [29]. This gelation mechanism, which results in the effects of the viscosity of the slurry being less pronounced at lower specific surface areas, may explain the higher recoveries of scheelite and hornblende (and the higher mass pull in general). The great ability of the gel structures to retain liquids could further explain the positive effects of the aluminate modification on water pull. On the other hand, the non-functionalized colloidal silica at a specific surface area of 500 m^2/g was subject to a coagulation mechanism due to its lower surface charge and the very small silica particles. The coagulation itself has much less influence on the viscosity of the pulp as compared to a gel network aggregation [17]. At a specific surface area of 250 m^2/g, the zeta potential at a pH of 8–10 is similar to that of silane-modified colloidal silica and appears to be stable against aggregation. The silane-modified colloidal silica, on the other hand, is much more stable to any form of aggregation, which is related to the fact that the silane layers provide a steric hindrance that effectively reduces interparticle attractive interactions and increases the stability of the dispersion. The effect of specific surface area/particle size of aluminate-modified silica particles is consistent with other observations that smaller nanoparticles lead to smaller froth bubbles and higher froth stability. This effect of specific surface area on mean bubble size is similar for the silane-modified colloidal silica. The non-functionalized colloidal silica, on the other hand, may undergo more compact aggregation due to lower repulsive forces and the fact that finer particles tend to coagulate more strongly than larger particles. Consequently, they may be forming larger coagulates, explaining the opposite effect of specific surface on the mean bubble size of the froth, with larger coagulates (finer particles/higher specific surface) leading to larger froth bubbles.

In the case of the silane-modified colloidal silica, the small effect of the specific surface area on the mean froth bubble size is explained by its high stability against aggregation and by the fact that its particles were

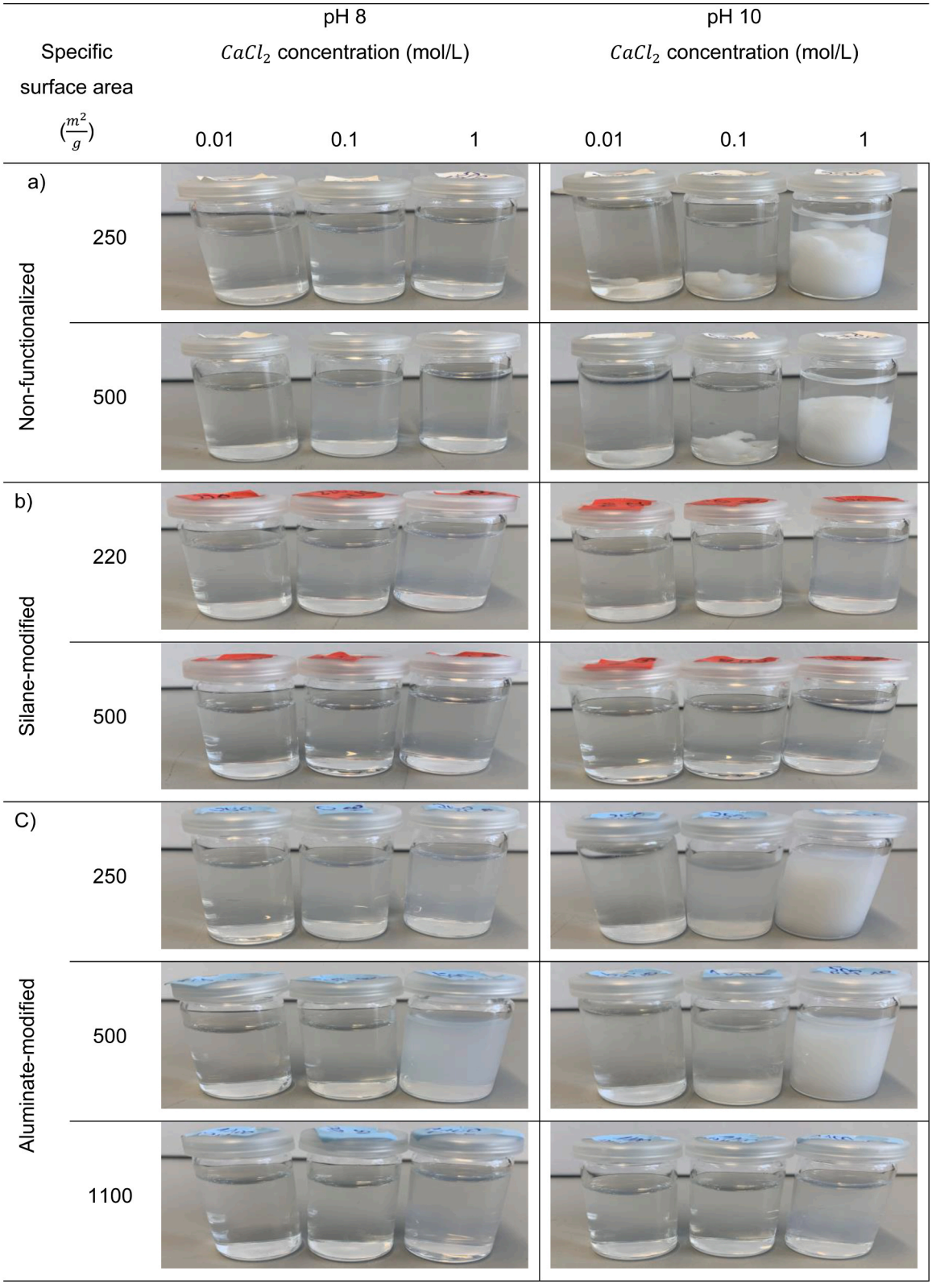


Fig. 19. Phase behavior of the Colloidal silica suspension depending on pH, specific surface area and $CaCl_2$ concentration for the non-functionalized (a), silane-modified (b), and aluminate-modified (c) colloidal silica.

not subject to any form of particle size growth. The very fine particles lead to the formation of very small froth bubbles and very stable froths. This froth structure then lends itself to better fluid drainage, resulting in slightly less water recovery as compared to standard colloidal silica.

Fig. 19 (Appendix II) shows the phase behavior of the dispersed silica nanoparticles at different $CaCl_2$ concentrations. Obviously, as the amount of $CaCl_2$ increases, the non-functionalized colloidal silica forms dense clumps in which the silica is more concentrated than in the initial sol so that the coagulate settles as a relatively dense precipitate. Instead, calcium chloride concentrations of 0.01 M and 0.1 M do not appear to be

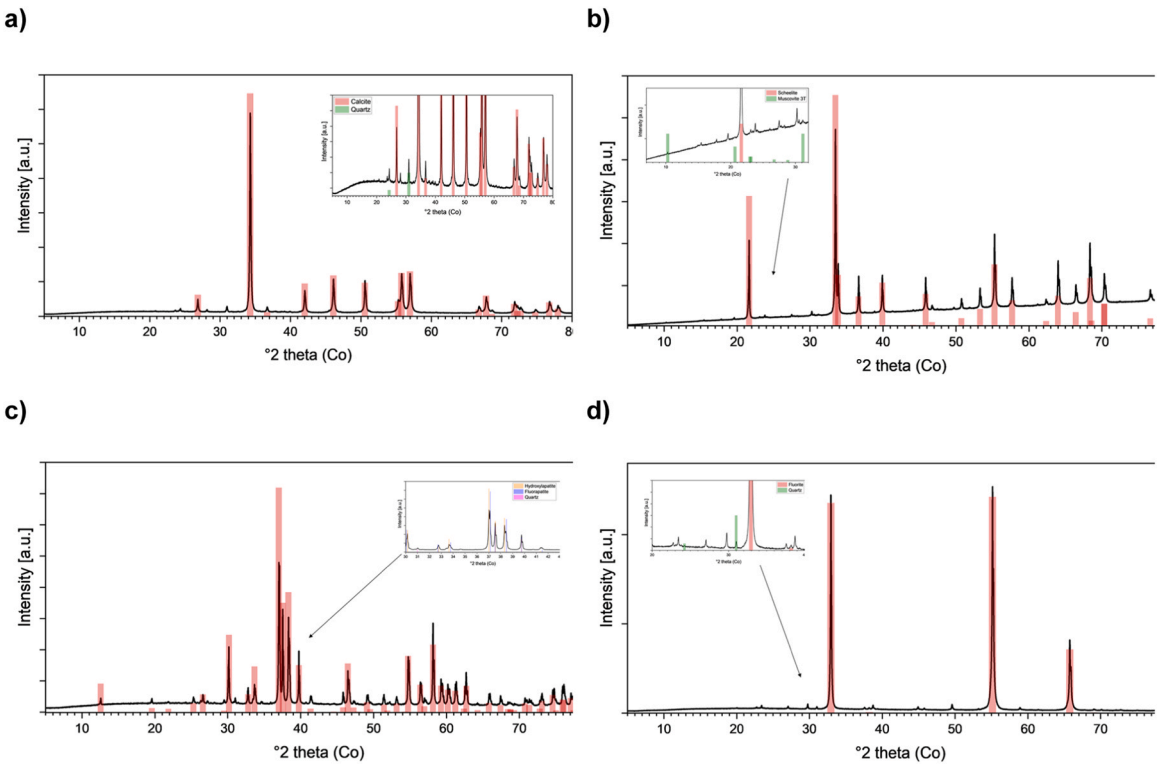


Fig. 20. Diffractograms obtained by X-ray diffraction (XRD) for calcite (a), scheelite (b), apatite (c) and fluorite (d).

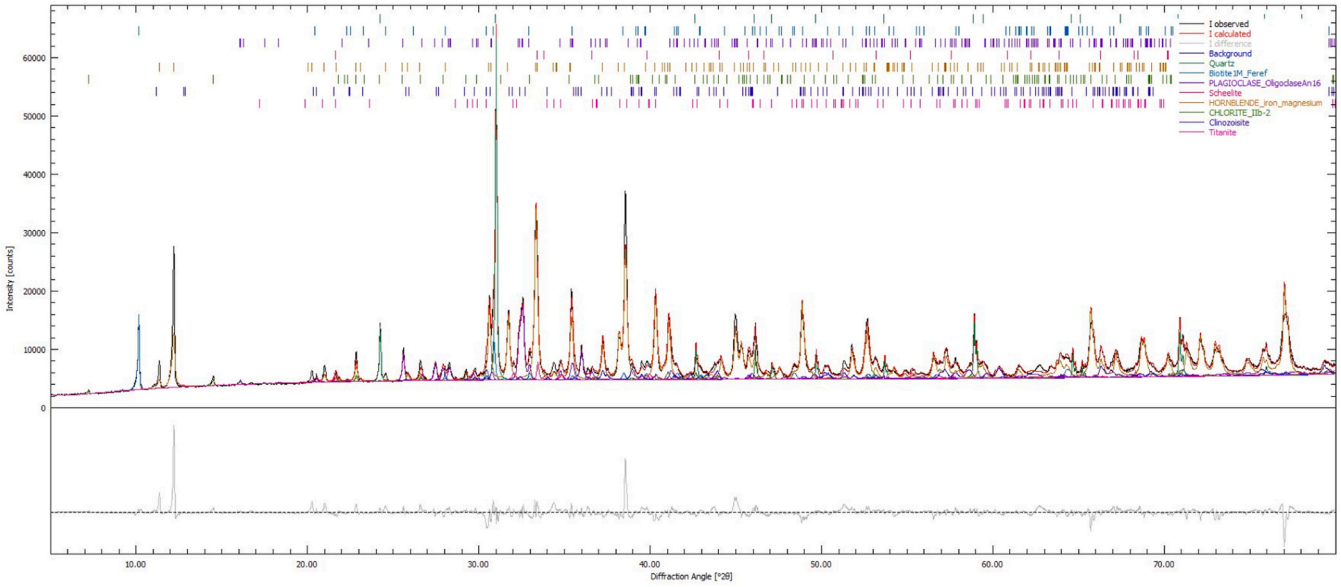


Fig. 21. Diffractogram obtained by X-ray diffraction (XRD) of the ore.

sufficient to destabilize the suspensions of aluminate-modified colloidal silica. No increase in silica concentration is observed in any macroscopic region of the medium, and only at high concentrations can the silica particles coalesce and form a coherent network that fills the entire volume. According to Kupka et al. [13], acidification of water glass causes it to depolymerize with high production of lower molecular weight silica species and form a gel over time depending on the acid used and the degree of acidification, as well as influencing the entrainment of gangue minerals, partly by affecting bubble coalescence in the pulp. With a high dosage of acid, the bubbles in the pulp tend to be smaller and the bubble coalescence in the froth is higher than with alkaline sodium silicate.

No observation was made for the silane-modified colloidal silica that could lead to any kind of particle aggregation. The proposed hypothesis and its link to the various effects on the overall flotation process are increasingly supported by these visually obtained observations.

Another reason could be that silane-modified colloidal silica has a lower zeta potential than non-functionalized and aluminate-modified silica. Huo et al. found that a low zeta potential is advantageous for the stability of colloidal froths and that an absolute value of the zeta

potential of 30 mV - 40 mV defines the boundary between stable and unstable froths [30]. It is also not excluded that the silane modification causes adequate hydrophobicity of the particles leading to the formation of a stable froth. This makes the effect of the specific surface area on the mean bubble size insignificant compared to non-functionalized and aluminate-modified colloidal silica. Although the hypothesis put forward appears to be plausible and is consistent with the most commonly observed effects, no definitive conclusion can yet be drawn due to the complexity of both the micro-processes in froth flotation and colloidal silica chemistry. An extended fundamental study, including the wettability and zeta potentials and surface forces of the various valuable and most importantly gangue mineral microparticles and how they are influenced by the effects of the various reagents and their interactions is under investigation.

4. Conclusion

We investigated the effect of colloidal silica on the microflotation of pure scheelite, calcite, apatite, and fluorite. In addition, colloidal silica was investigated as a calcite depressant in a laboratory-scale batch flotation for a low-grade scheelite ore. The experiments were carried out according to the design of experiments approach with varying the process parameters NaOl dosage, pH, CS dosage, CS modification, and CS specific surface area. Microflotation confirmed previous studies showing that colloidal silica depresses calcite. The recoveries of scheelite, apatite, and fluorite were not affected by the presence of the reagent. Batch flotation experiments showed significant differences in the effect of colloidal silica modification and specific surface area on the relevant target variables of mass and water pull, mean froth bubble size, and mineral recoveries. This phenomenon is thought to be due to differences in the aggregation mechanism between the various modifications of colloidal silica. While the sterically stabilized silane-modified colloidal silica does not appear to aggregate, the aluminate-modified and non-functionalized colloidal silica tend to aggregate in different forms: The non-functionalized colloidal silica tends to coagulate and form dense clumps, while the more stable aluminate-modified colloidal silica forms a gel network that is thought to affect the viscosity of the pulp. This leads to a reduction in mass pull on one side and an increase in water pull on the other, culminating in the formation of a less loaded foam. In contrast to the functionalized colloidal silicas, the less stable non-functionalized colloidal silica has the opposite effect of the specific surface area (i.e., particle size) on the median bubble size of the froth. This paved the way for a necessary extended fundamental investigation. Furthermore, the substantial enhancement in the scheelite-calcite selectivity index achieved by the addition of colloidal silica provides a promising outlook for its potential industrial applications. However, the application of this technology in an industrial context and the selection of the appropriate colloidal silica (including its modification, dosage, and specific surface area) require a multidimensional evaluation of the batch flotation results (mineral content and recovery) and the implementation of a systematic approach for upscaling the reagent system. These aspects are the main features of the forthcoming paper.

Declaration of Competing Interest

The authors declare that they have no known competing financial interests or personal relationships that could have appeared to influence the work reported in this paper.

Data availability

Data will be made available on request.

Acknowledgements

The authors would like to thank colleagues at Nouryon (formerly AkzoNobel Surface Chemistry, Sweden) for providing flotation reagents and meaningful discussions. The authors would like to thank many colleagues for their support with this project: Roland Würkert for sample preparation and Dr. Bradley Martin Guy for conducting the MLA analyses. This paper was written thanks to the financial support of the CoSilFlot project (03THWSN006) financed by the “WIPANO – Knowledge and Technology Transfer through Patents and Standards” a program of the German Federal Ministry of Economics and Energy (BMWi).

Appendix I. Element to Mineral Conversion (EMC)

This appendix outlines the procedure for converting chemical composition obtained with X-Ray Fluorescence into modal mineralogy by correlating with mineralogical data collected with mineral liberation analysis (MLA).

Elemental-to-mineral conversion methodologies

Elemental-to-mineral conversion (EMC) methods are based on simultaneously solving a set of linear algebraic equations formulated between chemical assays (b) and the chemical composition of minerals (A), to compute the mineralogical content of a material (x) (Eq.1). Eq.1 can be solved with the sum of least squares approach.

$$A * x = b \tag{1}$$

Methods and conversion scheme

Mineral Liberation Analysis

Automated mineralogy is based on the combination of high-resolution back-scattered electron and X-ray dispersive spectroscopy signals collected with a scanning electron microscope. This combination allows one to segment objects in a sample and identify their composing phases to conduct a thorough characterization of individual micrometer-sized particles in a sample in regarding their mineralogy. Automated mineralogy cannot be parametrized using analytical standards as typically done for techniques such as X-ray fluorescence. Yet, by comparing its modal mineralogy results with other techniques, the characterization results bias can be estimated. Samples in this study were analyzed with a Mineral Liberation Analyser, which has already been validated for their accuracy by the author.

Minerals subgroups

To simplify the conversion, minerals were grouped either by mineral class (e.g., chlorite and hornblende) or by similarities in chemical composition. A mineral that contains the total amount of a chemical element forms its own group (e.g., scheelite). Table 7 shows the subgroups and their constituent minerals and chemical elements and highlights the elements used for the EMC. The stoichiometric formula of each of these minerals was used to compute their composition.

Composition of multi-mineral subgroups

To compute the chemical formula of subgroups containing more than one mineral, the ratio between these minerals was used. Since some of these minerals behave differently in flotation, a specific ratio was used for the concentrate and tailings samples, as displayed in Table 8.

Flotation products can be divided into two classes that have almost the same flotation behavior, namely concentrates and tailings.

Chemical compositions of minerals

Samples belonging to the same sample class should generally have similar ratios of minerals in each subgroup. However, by changing the process conditions and the simplifications made during the conversion, these ratios should change somewhat, as should the chemical composition of the mineral matrix. This conversion matrix A' is then calculated using the solver shown in Fig. 17**.** As a constraint, the individual elements in the matrix A and A′ should not differ by more than 5%. This calculated matrix A′ is then used to calculate the modal mineralogy in the samples.

Conversion scheme

The conversion scheme used for each mineral class is shown in Fig. 18. From the contents of manganese (Mn) and potassium (K), the %w of ankerite and biotite are calculated. From this, the remaining amounts of calcium (Ca), magnesium (Mg), aluminum (Al) and iron (Fe) are calculated.

First, the talc content is calculated based on the chemical mass balance method by combining the %w of hornblende and biotite. In doing so, the solution targets the talc content so that the sum of the residuals of the measured and calculated talc contents is minimized. Once the talc content is calculated, its magnesium content is subtracted from the residual magnesium content and a new linear system is created to calculate the albite, chlorite and hornblende content. Once the hornblende content is determined, the residual calcium content that should be present in apatite, scheelite and calcite is calculated. After determining the apatite content from the %w of phosphorus and the scheelite content from the %w of tungsten, the residual calcium content %w is determined and the calcite content is calculated. Table 9 illustrates the conversion steps.

Appendix II

Fig. 19 shows the phase behavior of colloidal silica suspensions as a function of pH, CS modification and specific surface area, and $CaCl_2$ concentration.

Appendix III

Diffractograms obtained by X-ray diffraction (XRD) on a PANalytical Empyrean diffractometer with Co radiation at a voltage of 35 kV and a current of 35 mA for calcite (a), scheelite (b), apatite (c) and fluorite (d) are shown in Fig. 20**.**

The Diffractogram obtained by X-ray diffraction (XRD) on a PANalytical Empyrean diffractometer with Co radiation at a voltage of 35 kV and a current of 35 mA for the ore is shown in Fig. 21**.**

References

[1] B.A. Wills, J. Finch, Wills' Mineral Processing Technology - an Introduction to the Practical Aspects of Ore Treatment and Mineral Recovery, 2016512, https://doi.org/10.1016/B978-0-08-097053-0.00001-7..

[2] H. Yuehua, R. Chi, Z. Xu, Solution chemistry study of salt-type mineral flotation systems: role of inorganic dispersants, Ind. Eng. Chem. Res. 42 (8) (2003) 1641–1647, https://doi.org/10.1021/ie020729b.

[3] A. Faramarzpour, M.R. Samadzadeh Yazdi, B. Mohammadi, S. Chehreh Chelgani, Calcite in froth flotation - a review, J. Mater. Res. Technol. 19 (2022) 1231–1241, https://doi.org/10.1016/j.jmrt.2022.05.106.

[4] Z. Gao, C. Wang, W. Sun, Y. Gao, P.B. Kowalczuk, Froth flotation of fluorite: a review, Adv. Colloid Interface Sci. 290 (2021) 102–382, https://doi.org/10.1016/j.cis.2021.102382.

[5] C. Liu, Q. Feng, G. Zhang, W. Chen, Y. Chen, Effect of depressants in the selective flotation of scheelite and calcite using oxidized paraffin soap as collector, Int. J. Miner. Process. 157 (2016) 210–215, https://doi.org/10.1016/j.minpro.2016.11.011.

[6] Y. Foucaud, I.V. Filippova, L.O. Filippov, Investigation of the depressants involved in the selective flotation of scheelite from apatite, fluorite, and calcium silicates: Focus on the sodium silicate/sodium carbonate system, Powder Technol. 352 (2019) 501–512, https://doi.org/10.1016/j.powtec.2019.04.071.

[7] K.I. Marinakis, H.L. Shergold, Influence of sodium silicate addition on the adsorption of oleic acid by fluorite, calcite and barite, Int. J. Miner. Process. 14 (1985) 177–193, https://doi.org/10.1016/0301-7516(85)90002-X.

[8] W. Zhou, J. Moreno, R. Torres, H. Valle, S. Song, Flotation of fluorite from ores by using acidized water glass as depressant, Miner. Eng. 45 (2013) 142–145, https://doi.org/10.1016/j.mineng.2013.02.017.

[9] N. Kupka, M. Rudolph, Froth flotation of scheelite - a review, Int. J. Min. Sci. Technol. 28 (2018) 373–384, https://doi.org/10.1016/j.ijmst.2017.12.001.

[10] N. Kupka, R. Möckel, M. Rudolph, Acidified water glass in the selective flotation of scheelite from calcite, Part I: performance and impact of the acid type, Physicochem. Probl. Miner. Process. 56 (2020) 238–251, https://doi.org/10.5277/ppmp19101.

[11] L. Dong, F. Jiao, W. Qin, H. Zhu, W. Jia, Effect of acidified water glass on the flotation separation of scheelite from calcite using mixed cationic/anionic collectors, Appl. Surf. Sci. 444 (2018) 747–756, https://doi.org/10.1016/j.apsusc.2018.03.097.

[12] B. Feng, X. Luo, J. Wang, P. Wang, The flotation separation of scheelite from calcite using acidified sodium silicate as depressant, Miner. Eng. 80 (2015) 45–49, https://doi.org/10.1016/j.mineng.2015.06.017.

[13] N. Kupka, P. Kaden, A. Jantschke, E. Schach, M. Rudolph, Acidified water glass in the selective flotation of scheelite from calcite, Part II: species in solution and related mechanism of the depressant, Physicochem. Probl. Miner. Process. 56 (2020) 797–817, https://doi.org/10.37190/ppmp/125639.

[14] N. Kupka, B. Babel, D. Chinbat, M. Rudolph, Performance of acidified water glass in scheelite flotation against calcite, Flotation 17 (() (2017).

[15] M. Fuerstenau, G. Gutierrez, D.A. Elgillani, The influence of sodium silicate in nonmetallic flotation systems, Transactions 241 (1968) 319–323.

[16] A.I. Berlinskii, N.D. Klyueva, Interaction of alkaline and acidic water glass with some calcium minerals studied by infrared spectroscopic method, Obogashchenie Rud. 17 (1972) 16–18.

[17] R.K. Iler, The Chemistry of Silica, John Wiley & Sons, New York, 1979, p. 866.

[18] M.-S. Tsai, W.-C. Wu, Aluminum modified colloidal silica via sodium silicate, Mater. Lett. 58 (2004) 1881–1884, https://doi.org/10.1016/j.matlet.2003.12.006.
[19] M. Rasmusson and S. Wall, Electrostatic characterisation of Al-modified, nanosized silica particles, Colloids and Surfaces A: Physicochemical and Engineering Aspects, 122 169-181, https://doi.org/10.1016/S0927-7757(96)03850-2.
[20] B. Ben Said, L. Pereira, T. Saeed, D.H. Hoang, N. Kupka, R. Tolosana-Delgado, M. Rudolph, Development of a user-friendly R Platform for Optimizing Mineral Processing, Int. Miner. Process. Congr. Asia-Pac., Melb. Aust. (2022).
[21] B. Durakovic, Design of experiments application, concepts, examples: State of the art, Period. Eng. Nat. Sci. (PEN) 5 (2017), https://doi.org/10.21533/pen.v5i3.145.
[22] R. Fandrich, Y. Gu, D. Burrows, K. Moeller, Modern SEM-based mineral liberation analysis, Int. J. Miner. Process. 84 (2007) 310–320, https://doi.org/10.1016/j.minpro.2006.07.018.
[23] B. Ben Said, L. Pereira, R. Tolosana-Delgado, M. Rudolph, A Use -Friendly R. Platf. Optim. Miner. Process. (2022), https://doi.org/10.14278/rodare.1509.
[24] Open Source Computer Vision Library. (2015). [Online]. Available: https://github.com/itseez/opencv.
[25] R: A Language and Environment for Statistical Computing. (2022). R Foundation for Statistical Computing, Vienna, Austria. [Online]. Available: https://www.R-project.org/.
[26] I. Blute, R.J. Pugh, J. van de Pas, I. Callaghan, Silica nanoparticle sols 1. Surface chemical characterization and evaluation of the foam generation (foamability), J. Colloid Interface Sci. 313 (2007) 645–655, https://doi.org/10.1016/j.jcis.2007.05.013.
[27] S.H. Morar, D.J. Bradshaw, M.C. Harris, The use of the froth surface lamellae burst rate as a flotation froth stability measurement, Miner. Eng. 36-38 (2012) 152–159, https://doi.org/10.1016/j.mineng.2012.03.018.
[28] V.M. Kirjavainen, Mathematical model for the entrainment of hydrophilic particles in froth flotation, Int. J. Miner. Process. 35 (1992) 1–11, https://doi.org/10.1016/0301-7516(92)90002-E.
[29] X. Chen, E. Hadde, S. Liu, Y. Peng, The effect of amorphous silica on pulp rheology and copper flotation, Miner. Eng. 113 (2017) 41–46, https://doi.org/10.1016/j.mineng.2017.08.001.
[30] W. Huo, X. Zhang, K. Gan, Y. Chen, J. Xu, J. Yang, Effect of zeta potential on properties of foamed colloidal suspension, J. Eur. Ceram. Soc. 39 (2019) 574–583, https://doi.org/10.1016/j.jeurceramsoc.2018.08.035.